Synthesis, Properties, and Structure of a Stable Cobalt(III) Alkyl Peroxide Complex and Its Role in the Oxidation of Cyclohexane

Ferman A. Chavez,[†] Cattien V. Nguyen,[†] Marilyn M. Olmstead,[‡] and Pradip K. Mascharak*,[†]

Department of Chemistry and Biochemistry, University of California, Santa Cruz, California 95064, and Department of Chemistry, University of California, Davis, California 95616

Received May 8, 1996[⊗]

Three cobalt(III) complexes of Py_3PH_2 (H's are the dissociable amide H's), a strong-field ligand with two peptide groups, have been synthesized. They are $[Co(Py_3P)(H_2O)]ClO_4 \cdot H_2O$ (**6**), $[Co(Py_3P)(OH)]$ (**7**), and $[Co(Py_3P)(OO^t\text{-}Bu)] \cdot 2CH_2Cl_2$ (**8**). Complex **6** crystallizes in the monoclinic space group $C2$ with $a = 22.695(6)$ Å, $b = 10.284(2)$ Å, $c = 10.908(3)$ Å, $\alpha = 90°$, $\beta = 112.17(2)°$, $\gamma = 90°$, $V = 2357.7(10)$ Å^3, and $Z = 4$. Its structure has been refined to $R = 3.91\%$ on the basis of 1844 $I > 2\sigma(I)$ data. Complex **8** crystallizes in the monoclinic space group $P2_1/n$ with $a = 16.720(4)$ Å, $b = 10.641(3)$ Å, $c = 16.776(3)$ Å, $\alpha = 90°$, $\beta = 99.76(2)°$, $\gamma = 90°$, $V = 2941.5(12)$ Å^3, and $Z = 4$. The structure of **8** has been refined to $R = 6.37\%$ on the basis of 4776 $I > 2\sigma(I)$ reflections. In all three complexes, the doubly deprotonated Py_3P^{2-} ligand binds the cobalt(III) center in a pentadentate fashion with five nitrogens situated in two deprotonated amido groups and three pyridine rings. The aqua complex **6** can easily be converted into the hydroxo complex **7** by the addition of 1 equiv of base. The transformation **6** ↔ **7** is reversible, and the pK_a of the coordinated water molecule in **6** is 7. Complex **8** is the first example of a structurally characterized Co(III) alkyl peroxide complex that contains two deprotonated amido groups bonded to the metal center. Like a few alkyl peroxide complexes of tervalent cobalt, **8** oxidizes alkanes upon thermal decomposition. When cyclohexane is used as the substrate, cyclohexanol, cyclohexanone, and cyclohexyl chloride are the products. Complex **7** is the intermediate in the formation of **8** and is also the thermal decomposition product of **8**. In single turnover oxidation of cyclohexane by **8** at the optimum temperature of 80 °C, a maximum yield of 59% of the oxidized products is obtained. The mechanism of cyclohexane oxidation by **8** involves exclusive homolytic scission of the O−O bond in **8**. The ^{t}BuO$^\bullet$ radicals generated in such a process abstract an H atom from cyclohexane to afford cyclohexyl radicals, which in turn react with dioxygen and produce cyclohexanol and cyclohexanone presumably via a Russell-type termination reaction. The oxidation of cyclohexane by **8** can be either stoichiometric or catalytic. In the presence of excess TBHP, **8** affords more oxidized products, indicating multiple turnovers.

Introduction

Catalytic oxidation of hydrocarbons by transition metal salts (or complexes) and dioxygen represents one of the most important and challenging transformations in industrial chemistry.[1−5] Only a few systems are known to catalyze the C−H → C−OH transformation. One such example is the large-scale industrial production of adipic acid in which air oxidation of cyclohexane is accomplished in the presence of a cobalt catalyst. The reaction proceeds via a radical chain process involving cyclohexyl hydroperoxide. Cobalt plays a crucial role in controlling the conversion of this hydroperoxide to cyclohexanol and cyclohexanone.[2] Further radical-induced oxidation of cyclohexanone causes C−C bond cleavage, a process that affords adipic acid as the final product. It has been noted that homolyses of hydroperoxides are best promoted by cobalt (and manganese) salts and their complexes.[1] Thus cobalt is also employed in the Mid-Century/Amoco process for the production of terephthalic acid from *p*-xylene. This oxidation reaction is initiated by a Co(III) species.[1] The exact nature of the cobalt-containing intermediate in any of these industrial processes is unknown although Co(III) hydroperoxides have been postulated as intermediates on the basis of kinetic data.[6,7] Since the major function of the metal-containing species in many of the oxidation processes is modulation of the catalytic decomposition of alkyl (or aryl) hydroperoxides,[2] transient formation of cobalt alkyl peroxides and their decomposition along certain pathways could be important steps in the overall mechanism of the hydrocarbon oxidations. Therefore, studies on reactivities of discrete Co(III) alkylperoxy complexes toward hydrocarbons could provide insight into the nature and role of the cobalt-containing intermediate(s) in the hydrocarbon oxidation reactions.

Since low-spin d^6 Co(III) complexes are kinetically inert, Co(III)−peroxo complexes are amenable to isolation and characterization. While most of the peroxo complexes are binuclear, several mononuclear alkylperoxo complexes of tervalent cobalt are known. Among the Co(III) alkyl peroxides reported so far, $[Co(BPI)(OCOR)(OOR')]$ (**1**) (BPI = 1,3-bis(2-pyridylimino)-isoindoline); R = Me, Ph, ^{t}Bu; R′ = ^{t}Bu, $PhMe_2C$ (cumyl)),[8] $[Co(BPB)(OO^tBu)(4\text{-}Mepy)]$ (**2**) (BPB = *N*,*N*-bis(2-pyridin-

† University of California, Santa Cruz.
‡ University of California, Davis.
⊗ Abstract published in *Advance ACS Abstracts,* September 15, 1996.

(1) Ebner, J.; Riley, D. In *Active Oxygen in Chemistry*; Foote, C. S., Valentine, J. S., Greenberg, A., Liebman, J. F., Eds.; Chapman & Hall: London, 1995; pp 205−248.
(2) Parshall, G. W.; Ittel, S. D. In *Homogeneous Catalysis. The Applications and Chemistry of Catalysis by Soluble Transition Metal Complexes*, 2nd ed., Wiley-Interscience: New York, 1992.
(3) *Selective Hydrocarbon Activation*; Davies, J. A., Watson, P. L., Liebman, J. F., Greenberg, A., Eds.; VCH: New York, 1990.
(4) *Activation and Functionalization of Alkanes*; Hill, C. L., Ed.; Wiley-Interscience: New York, 1989.
(5) Sheldon, R. A.; Kochi, J. K. In *Metal-Catalyzed Oxidations of Organic Compounds*; Academic: New York, 1981.
(6) Bands, G. L.; Chalk, J. E.; Smith, J. F. *Nature* **1954**, *174*, 274.
(7) Black, J. F. *J. Am. Chem. Soc.* **1978**, *100*, 527.
(8) Saussine L.; Brazi, E.; Robine, A.; Mimoun, H.; Fischer, J.; Weiss, R. *J. Am. Chem. Soc.* **1985**, *107*, 3534.

S0020-1669(96)00500-9 CCC: $12.00

ecarboxamido)-1,2-benzene; 4-Mepy = 4-methylpyridine),[8] [Co(dmgH)$_2$(py)(OOR)] (**3**) (dmgH = monoanion of dimethylglyoxime; py = pyridine; R = ^{t}Bu),[9,10] and [Co(salen)(OOR)] (**4**) (salenH$_2$ = *N*,*N*-bis(salicyladehyde) ethylenediimine; R = ^{t}Bu)[11,12] are well-characterized. Also, the structures of [Co(BPI)(OCOPh)(OO^{t}Bu)] (**1**) R = ^{t}Bu; R′ = Ph; R″ = H),[8] [Co(dmgH)$_2$(py)(OOCMe$_2$Ph)] (**3**),[9] and the peroxy-*p*-quinolato adduct of a Schiff base complex of Co(III)[12] are known.

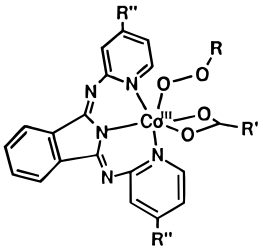

(1) R = ^{t}Bu, CMe$_2$Ph
R′ = Me, Ph, ^{t}Bu
R″ = H, Me

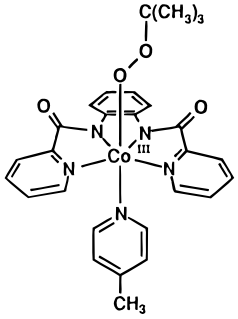

(2)

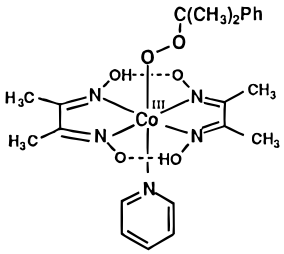

(3)

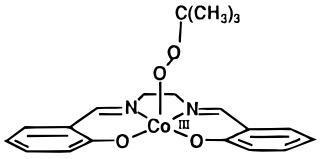

(4)

The ability of selected cobalt(III) alkyl peroxides to oxidize hydrocarbons has been investigated by Weiss and co-workers.[8] With the use of a series of Co(III) alkylperoxy complexes, this group has shown that reactivity toward hydrocarbons depends on the rates of thermal decomposition of the Co(III) alkyl peroxides. For example, [Co(BPI)(OCOMe)(OO^{t}Bu)] (**1b**) does not react with cyclohexane at room temperature but converts cyclohexane to cyclohexanol and cyclohexanone ((*tert*-butylperoxy)cyclohexane is the third product) at 60 °C or above. The BPI complexes are not only reactive in stoichiometric hydroxylation of alkanes but also catalytic in hydroxylation of alkanes by alkyl peroxides. In the catalytic oxidation of cyclohexane by cumene hydroperoxide and bis(acetylacetonato)cobalt(II), the Co(III)−cumylperoxo intermediate is also reactive at higher temperatures (above 60 °C).[13] These studies have revealed that the nature of the chelating ligand exerts a profound influence on the existence and stability of the Co(III)−alkylperoxo complexes. As a consequence, the rates of decomposition of the alkylperoxo complexes and the extent of alkane oxidation depend critically on the ligand(s) employed. Drago and coworkers have also demonstrated that ligand variation in a series of Co(II) Schiff base complexes affects their ability to catalyze the aerobic oxidation of phenolic substrates.[14]

In our attempts to (a) control the yields and product selectivity in alkane oxidation reactions by designed cobalt complexes and (b) establish the decomposition pathway of the catalysts, we have synthesized a pentadentate strong-field ligand (Py_3PH_2) (**5**), which has been utilized to synthesize [Co(Py_3P)(H_2O)]ClO_4·H_2O (**6**), [Co(Py_3P)(OH)] (**7**), and [Co(Py_3P)(OO^{t}Bu)]·2CH_2Cl_2 (**8**).

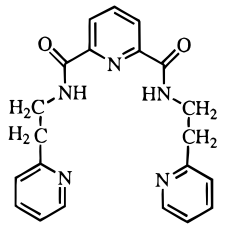

Py_3PH_2 (**5**)

The syntheses of Py_3PH_2 and its Cu(II) complex [Cu(Py_3P)] have been reported earlier.[15] In the entire set **6**−**8**, the ligand employs three pyridine nitrogens and two deprotonated amido nitrogens to bind Co(III). Complex **8** is the first example of a Co(III)−alkylperoxo complex that contains two deprotonated amido nitrogens ligated to cobalt and is capable of oxidizing alkanes stoichiometrically and catalytically under mild conditions. Complex **7** is an intermediate in the formation of **8** and the thermal decomposition product of **8**. In this paper, we describe the syntheses, structures, and properties of compounds **6** and **8** and synthesis and properties of **7**. The EPR parameters of the Co(II) complex [Co(Py_3P)] (**9**), which is an intermediate in the formation of **8**, and the interconversion of **6** to **7** are discussed. Optimization of conditions of alkane oxidation by **8**, distributions of the oxidized products, fate of the catalyst, and mechanism of alkane oxidation by **8** are also included.

Experimental Section

Materials. The ligand Py_3PH_2 (**5**) was synthesized by following the published procedure.[15] The strongly acidic cation exchanger SP-C50-120 was purchased from Sigma. Cobalt acetate tetrahydrate and lithium hydroxide hydrate were obtained from Alfa Products. Lithium perchlorate, cobalt(II) perchlorate hexahydrate, tetrafluoroboric acid (HBF_4, 48 wt % solution in water), 1,8-bis(dimethylamino)naphthalene, and *tert*-butyl hydroperoxide (TBHP) (90%) were procured from Aldrich Chemical Co. TBHP was further dried over anhydrous $MgSO_4$. Hydrogen peroxide (30%) was purchased from Fisher Scientific Co. The solvents were dried and distilled before use.

Synthesis. Safety Notes. *Caution!* Perchlorate salts of metal complexes with organic ligands are potentially explosive. Only small amounts of material should be prepared, and the compounds should be handled with great care.

Preparation of Compounds. [Co(Py_3P)(H_2O)]ClO_4·H_2O (6). The synthesis of **6** was carried out via H_2O_2 oxidation of a mixture of cobalt(II) acetate tetrahydrate and Py_3PH_2 in methanol. A batch of 334 mg (1.34 mmol) of cobalt(II) acetate tetrahydrate dissolved in 5 mL of methanol was slowly added to a solution of 503 mg (1.34 mmol) of Py_3PH_2 in 8 mL of methanol. To this mixture was added, after 5 min, 1.5 mL of 30% H_2O_2, followed by 2 equiv of NaOH dissolved in 8 mL of water. After 3 h of stirring, the volume of the mixture was reduced to 5 mL and the pH of the mostly aqueous solution was adjusted to 4 with dilute HBF_4. The sample was then loaded onto an SP-C50-120 Sephadex column (Na^+ form, 3 × 30 cm) and eluted with 0.1 N KCl, and the first green band was collected and dried. The KCl was removed by extracting the residue with dry ethanol. The green ethanolic extract was evaporated to dryness, and the resulting solid was redissolved in 20 mL of water. Three equivalents of $LiClO_4$ was added

(9) Giannotti, C.; Fontaine, C.; Chiaroni, A.; Riche, C. *J. Organomet. Chem.* **1976**, *113*, 57.
(10) Fontaine, C.; Duong, K. N. V.; Merienne, C.; Gaudemer, A.; Gianotti, C. *J. Organomet. Chem*. **1972**, *38*, 167.
(11) Nishinaga, A.; Tomita, H.; Ohara, H. *Chem. Lett.* **1983**, 1751.
(12) Nishinaga, A.; Tomita, H.; Nishizawa, K.; Matsuura, T.; Ooi, S.; Hirotsu, K. *J. Chem. Soc., Dalton Trans*. **1981**, 1505.
(13) Talsi, E. P.; Chinakov, V. D.; Babenko, V. P.; Sidelnikov, V. N.; Zamaraev, K. I. *J. Mol. Catal*. **1993**, *81*, 215.
(14) Corden, B. B.; Drago, R. S.; Perito, R. P. *J. Am. Chem. Soc.* **1985**, *107*, 2903.
(15) (a) Chavez, F. A.; Olmstead, M. M.; Mascharak, P. K. *Inorg. Chem.* **1996**, *35*, 1410. (b) A brief report on the same ligand and metal complexes derived therefrom was published by Nonoyama (Nonoyama, M. *Inorg. Chim. Acta* **1974**, *10*, 59); however, this account contained no physical or spectroscopic data on the ligand.

to this mixture, and the resultant greenish brown solution was filtered. Reddish-brown hexagonal plates were obtained upon slow diffusion of diethyl ether into the filtrate over 12 h. Yield: 319 mg (42%). ^{1}H NMR (303 K, D_2O, 500 MHz), δ (ppm from TSP): 2.11 (1H, t), 2.52 (1H, q), 3.16 (1H, d), 3.23 (1H, d), 3.45 (1H, t), 4.23 (1H, m), 4.35 (2H, m), 7.11 (1H, t), 7.20 (1H, d), 7.66 (1H, d), 7.72 (1H, t), 7.83 (2H, m), 8.05 (1H, d), 8.20 (1H, t), 8.31 (1H, d), 8.50 (1H, t), 9.57 (1H, d). ^{13}C NMR (303 K, D_2O, 125.58 MHz), δ (ppm from TSP): 38.72, 38.96, 41.80, 43.70, 126.77, 127.55, 128.50, 129.03, 130.47, 131.27, 143.64, 144.35, 145.83, 154.14, 158.17, 158.69, 158.90, 164.13, 166.97, 174.05, 175.24. Selected IR bands (KBr pellet, cm^{-1}): 3504 (m, br), 2918 (s), 2367 (m), 1590 (vs, ν_{CO}), 1475 (m), 1445 (s), 1400 (s), 1338 (m), 1305 (s), 1252 (w), 1160 (w), 1094 (vs, $\nu(ClO_4^-)$), 839 (m), 770 (s), 680 (w), 622 (s), 600 (m), 466 (m). Electronic absorption data [λ_{max}, nm (ϵ, M^{-1} cm^{-1})]: in water 588 (73), 325 (sh, 6000), 270 (sh, 15 000), 245 (sh, 23 000); in methanol 638 (90), 265 (20 000).

[Co(Py$_3$P)(OH)] (7). A solution of 13.4 mg (0.32 mmol) of LiOH·H_2O in 2 mL of MeOH was added to a slurry of 181.6 mg (0.32 mmol) of **6** in 10 mL of dicholoromethane. Most of the solid dissolved within a few minutes, and a red solution resulted. After 2 h of stirring, 3 mL of diethyl ether was added, and the solution was filtered. The filtrate was then stored at 4 °C. Reddish-brown crystals of **7** were isolated from this solution after 12 h. Yield: 50.3 mg (35.8%). ^{1}H NMR (303 K, D_2O, 500 MHz), δ (ppm from TSP): 2.24 (1H, t), 2.47 (1H, q), 3.00 (1H, d), 3.15 (1H, d), 3.28 (1H, t), 4.16 (3H, m), 7.11 (1H, t), 7.20 (1H, d), 7.56 (1H, d), 7.70 (1H, d), 7.75 (1H, t), 8.12 (1H, t), 8.20 (1H, d), 8.39 (1H, t), 9.49 (1H, d). Selected IR bands (KBr pellet, cm^{-1}): 3423 (s), 3070 (m), 2959 (m), 1596 (vs, ν_{CO}), 1478 (m), 1443 (s), 1389 (s), 1336 (m), 1301 (s), 1250 (w), 1194 (w), 1162 (w), 1114 (w), 1085 (w), 1040 (w), 837 (w), 769 (s), 740 (w), 681 (m), 596 (w). Electronic absorption spectrum in water [λ_{max}, nm (ϵ, M^{-1} cm^{-1})]: 560 (sh, 60), 317 (1400), 260 (sh, 10 000).

[Co(Py$_3$P)(OO^{t}Bu)]·2CH$_2$Cl$_2$ (8). A mixture of 1.054 g (2.81 mmol) of Py_3PH_2, 1.028 g of (2.81 mmol) of $Co(ClO_4)_2$·$6H_2O$, and 1.204 g (5.62 mmol) of 1,8-bis(dimethylamino)naphthalene in 15 mL of methanol was stirred for 1 h under dry dinitrogen. The burgundy-colored solution of [Co(Py$_3$P)] was then filtered, and the methanol was removed under vacuum. The residue was resuspended in 10 mL of dicholoromethane, and 1.97 mL (7 equiv) of dry ^{t}BuOOH was added to the suspension. The resulting deep green solution was stirred for 30 min, 20 mL of diethyl ether was then added, and the resulting solution was allowed to stand at 4 °C. Black crystals of **8** were deposited within 48 h. Yield: 687 mg (35%). Recrystallization of the initial product from dicholoromethane/diethyl ether afforded crystals that were suitable for X-ray analysis. ^{1}H NMR (298 K, $CDCl_3$, 500 MHz), δ (ppm from TMS): 0.52 (9H, ^{t}Bu), 2.20 (1H, t), 2.45 (1H, q), 2.77 (1H, q), 2.95 (1H, d), 3.19 (1H, t), 3.94 (1H, q), 4.22 (2H, m), 6.97 (2H, m), 7.31 (1H, d), 7.52 (2H, m), 7.81 (1H, m), 7.90 (1H, t), 8.03 (2H), 8.24 (1H, d), 9.58 (1H, d). ^{13}C NMR (298 K, $CDCl_3$, 125.58 MHz), δ (ppm from TMS): 26.55 (CH_3, ^{t}Bu) 36.02, 37.13, 39.46, 39.91, 75.97 (C, ^{t}Bu), 122.35, 122.50, 122.55, 122.83, 127.00, 138.49, 138.80, 150.47, 156.44, 157.30, 157.64, 161.75, 163.36, 170.17, 170.74. Selected IR bands (KBr pellet, cm^{-1}): 3418 (s, br), 2973 (s), 2919 (s), 2861 (s), 1590 (vs, ν_{CO}), 1475 (s), 1451(s), 1388 (s), 1355 (s), 1331 (m), 1301 (s), 1192 (s), 1114 (m), 1043 (m), 879 (m, ν_{OO}), 772 (s), 678 (m), 594 (m), 531 (w), 488 (w), 464 (m). Electronic absorption data recorded in dichloromethane [λ_{max}, nm (ϵ = M^{-1} cm^{-1})]: 645 (212), 248 (20 000).

Other Physical Measurements. Infrared spectra were obtained with a Perkin-Elmer 1600 FTIR spectrophotometer, absorption spectra were measured on a Perkin-Elmer Lambda 9 spectrophotometer, a Bruker ESP-300 spectrometer was used to record the EPR spectra at X-band frequencies, and ^{1}H and ^{13}C NMR spectra were recorded on a Varian 500 MHz Unity Plus instrument interfaced with a Sun OS 4.1.3 computer. Standard organic product analyses were performed on a Hewlett-Packard 5890 Series II Plus gas chromatograph equipped with a flame-ionization detector (FID) and Heliflex AT-1701 (30 m × 0.25 mm o.d.; film thickness 0.25 μm) capillary column (Alltech). Satisfactory analyses were obtained for all the complexes.

Oxidation of Hydrocarbon Substrates. In a typical oxidation experiment, 30−35 μmol of **8** was dissolved in 1 mL of 1:1 v/v dichloromethane/cyclohexane in a 2 dram screw cap vial with a Teflon seal. The vial was weighed and then immersed in a water bath of the desired temperature. After the desired time period, the reaction mixture was quickly cooled to room temperature and weighed to determine if a portion of the mixture had been lost. The reaction mixture was then filtered through a 0.45 μm Acrodisc Nylon filter. A known amount of toluene (internal standard) was added to the filtrate, and the mixture was injected into the gas chromatograph. Retention times for product peaks were compared directly with those of known standard compounds. The yields were calculated using proper correction factors. For catalytic oxidations, 35 μmol of **8** (or **7**) and 100 μL of TBHP were dissolved in 1 mL of 1:1 v/v dichloromethane/cyclohexane in a 2 dram screw cap vial with a Teflon seal. Reactions and product analyses were carried out as indicated above.

X-ray Data Collection and Structure Solution and Refinement. Reddish-brown hexagonal plates of **6**, suitable for X-ray analysis, were obtained by slow diffusion of diethyl ether into an aqueous solution of **6**. Black parallelepipeds of **8** were obained by cooling a solution of the complex in a dicholoromethane/diethyl ether mixture at 4 °C. The X-ray data were collected with a Siemens R3m/V diffractometer at room temperature for **6** and at 130 K for **8**. Only random fluctuations of <1.0% in the intensities of two standard reflections were observed during data collection. All calculations were carried out on a 486/DX50 computer using the SHELXTL Version 5.03 program.[16]

The structure of **6** was solved in the space group *C*2 by direct and difference Fourier methods. The alternative space groups, *Cm* and *C*2/*m*, are not possible, given the point symmetry of the molecule. The handedness was determined by use of the Flack parameter. Two hydrogens for the coordinated water molecule were located on a difference map late in the refinement; their positional parameters were fixed as found, and their isotropic thermal parameters were fixed at 0.04 Å^2. The perchlorate anion is disordered in two equal sites differing in relative rotation and shifted by 0.72 Å from chlorine to chlorine. This was modeled using distance constraints (DFIX) for Cl−O and O···O separations. For the noncoordinated water molecules, the two sites separated by 1.13 Å were identified and the oxygen atoms were arbitrarily assigned 0.5 occupancy. Their hydrogen atoms were not located. Hydrogen atoms bonded to carbon and nitrogen were added geometrically and refined with a riding model. An absorption correction (XABS2)[17] was applied. In the final cycles of refinement, all non-hydrogen atoms except those of the above disorder were refined with anisotropic thermal parameters. Refinement was carried out using all data, based on F^2. The largest feature in the final difference map had a peak value of 0.26 e Å^{-3}, 1.08 Å from O7B of the disordered perchlorate. The structure of **8** was solved in the monoclinic space group $P2_1/n$ using direct and difference Fourier methods. The bonded peroxide is disordered into two sets of atoms except for C25, which is shared. Disordered atoms of the same type were refined with common thermal parameters. Set A has 0.758(4) occupancy; set B has 0.242(4) occupancy. Loose distance restraints were applied that set the Co−O, C−C, and O−C distances equal to within 0.03 Å and the O−O distances equal to within 0.04 Å for the atoms of the disordered peroxide moiety. These atoms were refined with isotropic thermal parameters. In the final cycles of refinement, all non-hydrogen atoms except those of the above disorder were refined with anisotropic thermal parameters. Hydrogen atoms bonded to carbon and nitrogen were added geometrically and refined with a riding model. An absorption correction (XABS2)[17] was also applied.

Machine parameters, crystal data, and data collection parameters are summarized in Table 1. Positional coordinates are included in Tables 2 and 3, while selected bond distances and angles are listed in Table 4. The two sets of crystallographic data have been submitted as Supporting Information.

(16) G. Sheldrick (1995). Distributed by Siemens Industrial Automation, Inc., Madison, WI. Tables of neutral-atom scattering factors, *f′* and *f″*, and absorption coefficients were taken from: *International Tables for Crystallography*; Wilson, A. J. C., Ed.; Kluwer Academic Publishers: Dordrecht, The Netherlands, 1992; Vol. C, Tables 6.1.1.3 (pp 500−502), 4.2.6.8 (pp 219−222), and 4.2.4.2 (pp 193-199), respectively.

(17) XABS2: Parkin, S. R.; Moezzi, B.; Hope, H. *J. Appl. Crystallogr.* **1995**, *28*, 53.

Table 1. Summary of Crystal Data and Intensity Collection and Structure Refinement Parameters for $[Co(Py_3P)(H_2O)]ClO_4 \cdot H_2O$ (**6**) and $[Co(Py_3P)(OO^tBu)] \cdot 2CH_2Cl_2$ (**8**)

	complex **6**	complex **8**
formula	$C_{21}H_{23}N_5O_8ClCo$	$C_{27}H_{32}N_5O_4Cl_4Co$
mol wt	567.81	691.31
cryst color, habit	red-brown plate	black parallelepiped
T, K	298	130
cryst system	monoclinic	monoclinic
space group	$C2$	$P2_1/n$
a, Å	22.695(6)	16.720(4)
b, Å	10.284(2)	10.641(3)
c, Å	10.908(3)	16.776(3)
α, deg	90	90
β, deg	112.17(2)	99.76(2)
γ, deg	90	90
V, Å^3	2357.7(10)	2941.5(12)
Z	4	4
d_{calcd}, g cm^{-3}	1.594	1.561
abs coeff, μ, mm^{-1}	0.899	0.990
GOF[a] on F^2	0.947	1.017
R1,[b] %	3.91	6.37
wR2,[c] %	9.78	13.73

[a] GOF $= [\sum[w(F_o^2 - F_c^2)^2]/(M - N)]^{1/2}$ (M = number of reflections, N = number of parameters refined). [b] R1 $= \sum||F_o| - |F_c||/\sum|F_o|$. [c] wR2 $= [\sum[w(F_o^2 - F_c^2)^2]/\sum[w(F_o^2)^2]]^{1/2}$.

Results and Discussion

Syntheses of Co(III) complexes are usually achieved by aerobic or chemical oxidation of mixtures of Co(II) salts and the appropriate ligands. These reactions often proceed via Co(III)−superoxo or binuclear μ-peroxo intermediates.[18] In the present study, $[Co(Py_3P)(H_2O)]ClO_4 \cdot H_2O$ (**6**) has been synthesized via chemical (H_2O_2) oxidation of a mixture of Co(II) acetate and Py_3PH_2 in aqueous methanol. Ligation of the deprotonated amido nitrogens to Co(III) occurs only when 2 equiv of a strong base is added. The dark brown reaction mixture affords at least two distinct bands, one reddish brown (first band) and one greenish brown (second band), upon passage through a SP-C50-120 sephadex column. Crystals of **6** are obtained from the second band after desalting and further workup. In earlier attempts, it was discovered that the amounts of cobalt-containing species in the two bands depend critically on the pH of the reaction mixture. More complex **6** is obtained when the pH of the reaction mixture is maintained around 5. Since the cobalt-containing species in the first (reddish brown) band does not bind to the cation exchange column material and comes out of the column quite rapidly, it became apparent that the complex must be a neutral one. Further work confirmed this prediction, and the hydroxo complex $[Co(Py_3P)(OH)]$ (**7**) was isolated from band 1 in moderate yield. Once deprotonation of the coordinated water molecule of complex **6** was identified as the source of band 1 (i.e. complex **7**), better synthetic methods were developed. One obtains a much higher yield of complex **7** along with **6** if the pH of the initial reaction mixture that affords **6** is maintained above 8. Alternatively, complex **7** can be synthesized in pure crystalline form by the addition of 2 equiv of LiOH (or R_4NOH) to a slurry of **6** in dichloromethane.

The starting material for $[Co(Py_3P)(OO^tBu)] \cdot 2CH_2Cl_2$ (**8**) is the Co(II) complex $[Co(Py_3P)]$ (**9**). Reaction of $Co(ClO_4)_2 \cdot 6H_2O$ with Py_3PH_2 in methanol in the presence of 2 equiv of 1,8-bis(dimethylamino)naphthalene affords **9** in almost quantitative yield. 1,8-Bis(dimethylamino)naphthalene is the most convenient base for the above reaction, since the perchlorate salt of 1,8-bis(dimethylamino)naphthalene is insoluble in methanol and therefore can be conviently separated from the burgundy colored solution of **9**. Removal of methanol affords **9** in pure microcrystalline form. When **9** is dissolved in dichloromethane under dry nitrogen and excess TBHP is added, the solution immediately turns green due to oxidation of the Co(II) center to Co(III). The *tert*-butylperoxo complex **8** is obtained from this green solution upon addition of diethyl ether and storage at 4 °C.

Table 2. Atomic Coordinates ($\times 10^4$) and Equivalent Isotropic Displacement Parameters (Å $\times 10^3$) for $[Co(Py_3P)(H_2O)](ClO_4) \cdot H_2O$ (**6**)

	x	y	z	U(eq)[a]
Co	−1928(1)	−2523(1)	7057(1)	35(1)
O1	−3286(2)	201(5)	5681(5)	49(1)
O2	−2328(2)	−6323(5)	6808(4)	48(1)
O3	−1928(2)	−2601(6)	5275(3)	38(1)
N1	−1065(2)	−1802(6)	7537(5)	45(2)
N2	−2306(3)	−813(6)	6730(5)	39(1)
N3	−2778(3)	−3036(6)	6312(5)	35(1)
N4	−1786(3)	−4373(6)	7273(5)	39(1)
N5	−1886(2)	−2601(8)	8879(4)	42(1)
C1	−667(3)	−2459(11)	7093(6)	52(2)
C2	−72(3)	−1977(10)	7274(8)	68(2)
C3	122(3)	−786(10)	7877(9)	66(3)
C4	−289(4)	−112(9)	8270(8)	63(2)
C5	−892(4)	−611(8)	8087(7)	49(2)
C6	−1372(4)	181(9)	8415(8)	54(2)
C7	−1984(4)	432(8)	7233(7)	46(2)
C8	−2938(4)	−785(8)	6051(8)	41(2)
C9	−3212(3)	−2126(7)	5796(6)	38(2)
C10	−3838(3)	−2478(11)	5112(6)	46(2)
C11	−3988(3)	−3783(8)	5010(7)	47(2)
C12	−3525(3)	−4733(8)	5540(7)	43(2)
C13	−2895(3)	−4305(8)	6176(7)	34(2)
C14	−2306(3)	−5094(8)	6776(7)	40(2)
C15	−1216(4)	−4966(9)	8252(8)	52(2)
C16	−944(3)	−4062(8)	9457(7)	53(2)
C17	−1437(3)	−3336(7)	9801(6)	44(2)
C18	−1433(4)	−3407(9)	11080(7)	59(2)
C19	−1874(4)	−2702(12)	11423(7)	68(3)
C20	−2331(4)	−2048(9)	10468(7)	62(2)
C21	−2324(3)	−2014(8)	9225(7)	51(2)
ClA	837(2)	2620(6)	8216(4)	64(1)
O4A	1241(7)	3630(15)	8499(16)	80(5)
O5A	284(7)	2506(21)	6971(13)	87(4)
O6A	458(9)	2827(21)	9114(16)	110(6)
O7A	1210(9)	1488(21)	8306(19)	120(6)
ClB	584(2)	3093(5)	7965(4)	59(1)
O4B	168(7)	4137(18)	7469(16)	114(5)
O5B	1161(6)	3665(14)	7849(14)	72(4)
O6B	434(7)	1931(16)	7100(15)	82(4)
O7B	759(8)	2669(21)	9341(14)	98(5)
O8	−4557(10)	507(27)	5660(22)	153(8)
O9	−4331(12)	1496(33)	5723(24)	176(9)

[a] U(eq) is defined as one-third of the trace of the orthogonalized $\mathbf{U}_{ij}$ tensor.

Structure of $[Co(Py_3P)(H_2O)]ClO_4 \cdot H_2O$ (6). The structure of the cation of **6** is shown in Figure 1, while selected bond distances and bond angles are listed in Table 4. The coordination geometry around cobalt is octahedral with two deprotonated amido nitrogens and two pyridine nitrogens in the equatorial plane. The axial positions are occupied by a pyridine and a H_2O molecule. As is the case with $[Cu(Py_3P)]$,[15a] **6** contains a long, a medium, and a short $M-N_{py}$ (py = pyridine) bond, Co−N1 (1.972(6) Å), Co−N5 (1.955(5) Å), and Co−N3 (1.864(5) Å), respectively. The Co−N3 bond exerts a considerable trans effect which lengthens the Co−N1 bond. The $Co-N_{amido}$ distance of **6** (1.930(6) Å) is well within the range of the $Co-N_{amido}$ distances noted for other similar Co(III)−peptido com-

(18) Cotton, F. A.; Wilkinson, G. *Advanced Inorganic Chemistry*, 5th ed.; Wiley; New York, 1988; pp 735−738.

Table 3. Atomic Coordinates ($\times 10^4$) and Equivalent Isotropic Displacement Parameters (Å $\times 10^3$) for $[Co(Py_3P)(OO^tBu)]\cdot 2CH_2Cl_2$ (**8**)

	x	*y*	*z*	*U*(eq)[a]
Co	2199(1)	−93(1)	46(1)	18(1)
O1	4077(2)	−2022(3)	1259(2)	27(1)
O2	1463(2)	−529(3)	−2352(2)	28(1)
O3A	1484(4)	−1401(5)	236(4)	26(1)
O4A	1938(2)	−2435(4)	746(2)	26(1)
O3B	1489(14)	−1365(14)	354(12)	26(1)
O4B	1535(7)	−2515(11)	−66(7)	26(1)
N1	1626(2)	932(3)	740(2)	20(1)
N2	3046(2)	−566(3)	916(2)	20(1)
N3	2714(2)	−1258(3)	−513(2)	19(1)
N4	1543(2)	156(3)	−1026(2)	21(1)
N5	2835(2)	1371(3)	−296(2)	20(1)
C1	811(3)	951(4)	561(3)	26(1)
C2	323(3)	1616(4)	1001(3)	31(1)
C3	699(3)	2275(5)	1665(3)	35(1)
C4	1538(3)	2221(4)	1884(3)	32(1)
C5	1998(3)	1534(4)	1411(3)	25(1)
C6	2894(3)	1371(4)	1670(3)	26(1)
C7	3130(3)	−19(4)	1723(2)	25(1)
C8	3515(2)	−1516(4)	779(2)	23(1)
C9	3308(2)	−1943(4)	−91(2)	22(1)
C10	3649(3)	−2922(4)	−467(3)	24(1)
C11	3355(3)	−3159(4)	−1276(3)	27(1)
C12	2730(2)	−2427(4)	−1699(2)	25(1)
C13	2402(2)	−1479(4)	−1288(2)	22(1)
C14	1739(2)	−571(4)	−1615(3)	23(1)
C15	1111(3)	1321(4)	−1287(3)	27(1)
C16	1555(3)	2451(4)	−854(3)	27(1)
C17	2468(3)	2348(4)	−740(2)	26(1)
C18	2917(3)	3228(4)	−1079(3)	33(1)
C19	3753(3)	3130(5)	−978(3)	36(1)
C20	4125(3)	2149(5)	−530(3)	32(1)
C21	3650(3)	1294(4)	−199(2)	26(1)
C22	1511(3)	−3595(4)	527(3)	33(1)
C23A	1434(4)	−3897(7)	−365(4)	39(1)
C24A	2112(4)	−4563(6)	1006(4)	39(1)
C23B	1466(13)	−4704(17)	−25(12)	39(1)
C24B	2187(11)	−3478(21)	1203(11)	39(1)
C25	699(3)	−3555(5)	822(3)	42(1)
Cl1	3967(1)	4179(1)	2548(1)	37(1)
Cl2	4463(1)	4380(1)	965(1)	44(1)
C26	4479(3)	5109(5)	1915(3)	32(1)
Cl3A	3758(4)	520(4)	−2542(2)	60(1)
Cl4A	4912(2)	−1521(3)	−2115(3)	39(1)
C27A	4455(4)	−178(8)	−1789(5)	34(2)
Cl3B	3487(5)	246(8)	−2404(5)	33(2)
Cl4B	4891(7)	−1379(11)	−1847(7)	46(3)
C27B	4484(11)	208(18)	−2229(13)	19(5)
Cl3C	4008	595	−2884	40
Cl4C	4804	−1083	−1608	40
C27C	4775	−29	−2385	40

[a] *U*(eq) is defined as one-third of the trace of the orthogonalized $\mathbf{U}_{ij}$ tensor.

plexes (1.915−1.935 Å).[19−23] Also, the Co−OH_2 distance in **6** (1.945(4) Å) is identical to the Co−OH_2 distance in $[Co^{III}(PMA)(H_2O)]^+$, a Co(III)-bleomycin analogue that also contains an axially ligated water molecule.[22] The two deprotonated peptide moieties and the central pyridine are part of two five-membered chelate rings. Deviations from ideal octahedral geometry can be seen by the N2−Co−N4 and N3−Co−N1 angles (164.4(2) and 169.4(2)°, respectively). The N5−Co−O3 bond angle (174.7(3)°) is however closer to the ideal value of 180°. The pyridine ring containing N1 is tilted 42° relative to the pyridine ring containing N3 along the Co−N1 axis.

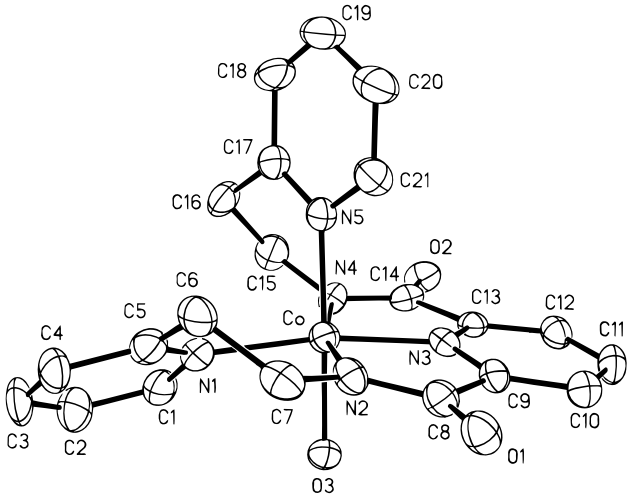

Figure 1. Computer-generated thermal ellipsoid (probability level 35%) plot of $[Co(Py_3P)(H_2O)]^+$ (cation of **6**) with the atom-labeling scheme. Hydrogen atoms are omitted for clarity.

Structure of $[Co(Py_3P)(OO^tBu)]\cdot 2CH_2Cl_2$ (8). The structure of **8** is illustrated in Figure 2, and selected bond distances and bond angles are included in Table 4. As seen in Figure 2, the mode of ligation of the doubly deprotonated Py_3P^{2-} ligand to the Co(III) center in **8** is very similar to that in **6**. The coordination geometry around the cobalt is distorted octahedral with two deprotonated amido nitrogens and two pyridine ring nitrogens in the equatorial positions while a $^tBuOO^-$ group and a pyridine molecule occupy the axial positions. Complex **8** also has long, medium, and short Co−N_{py} bonds, Co−N5 (2.024(3) Å), Co−N1 (1.960(3) Å), and Co−N3 (1.852(3) Å), respectively. The two deprotonated amido nitrogens, N2 and N4, and the central pyridine ring nitrogen, N3, form two adjacent five-membered chelate rings. The two pyridine rings containing N1 and N3 are positioned 37.5° to each other. Although the $^tBuOO^-$ group is somewhat disordered, molecular parameters based on the model can be used for comparison purposes. The Co−O3 bond length of **8** (weighted average 1.905(6) Å) is well within the range of Co−O distances noted in other alkylperoxo complexes of tervalent cobalt (1.838(5)−1.909(3) Å).[8,9,12] Also, the O3−O4 bond length (weighted average 1.49(5) Å) is comparable to the O−O bond lengths of other Co(III) alkylperoxo complexes (1.44(6)−1.50(1) Å).[8,9,12] The angles at the two oxygen atoms of the coordinated $^tBuOO^-$ group (Table 4) are consistent with sp^3-hybridized oxygen atoms.

Properties. At room temperature, the alkylperoxo complex **8** is relatively stable in the solid state but decomposes readily in aqueous solution (as indicated by the loss of color). The stability is clearly superior in halogenated hydrocarbons. For example, in chloroform solution, **8** is stable for at least 48 h whereas, in dichloromethane, it stays intact for about 1 week. The stability of **8** in such solvents is greatly improved in the presence of excess TBHP.

Ligation of the deprotonated amido nitrogens to Co(III) in all three complexes (**6**−**8**) is evident in their IR spectra. Free

(19) Farinas, E. F.; Tan, J. D.; Baidya, N.; Mascharak, P. K. *J. Am. Chem. Soc.* **1993**, *115*, 2996.
(20) Tan, J. D.; Hudson, S. E.; Brown, S. J.; Olmstead, M. M.; Mascharak, P. K. *J. Am. Chem. Soc.* **1992**, *114*, 3841.
(21) Muetterties, M.; Cox, M. B.; Arora, S. K.; Mascharak, P. K. *Inorg. Chim. Acta* **1989**, *160*, 123.
(22) Brown, S. J.; Hudson, S. E.; Olmstead, M. M.; Mascharak, P. K. *J. Am. Chem. Soc.* **1989**, *111*, 6446.
(23) Delany, K.; Arora, S. K.; Mascharak, P. K. *Inorg. Chem.* **1988**, *27*, 705 and references cited therein.
(24) (a) Guajardo, R. J.; Chavez, F.; Farinas, E. T.; Mascharak, P. K. *J. Am. Chem. Soc.* **1995**, *117*, 3883. (b) Guajardo, R. J.; Hudson, S. E.; Brown, S. J.; Mascharak, P. K. *J. Am. Chem. Soc.* **1993**, *115*, 7971. (c) Guajardo, R. J.; Tan, J. D.; Mascharak, P. K. *Inorg. Chem.* **1994**, *33*, 2838. (d) Brown, S. J.; Olmstead, M. M.; Mascharak, P. K. *Inorg. Chem.* **1990**, *29*, 3229.

Table 4. Selected Bond Distances (Å) and Angles (deg)

$[Co(Py_3P)(H_2O)]ClO_4 \cdot H_2O$ (**6**)

Bond Distances

Co−N1	1.972(6)	N2−C8	1.344(9)
Co−N2	1.930(6)	N3−C13	1.330(10)
Co−N3	1.864(5)	N4−C14	1.323(10)
Co−N4	1.929(6)	N4−C15	1.464(9)
Co−N5	1.955(5)	N5−C17	1.360(9)
Co−O3	1.945(4)	C8− O1	1.255(10)
N1−C5	1.355(10)	C14−O2	1.266(10)
N2−C7	1.437(9)	C19−C20	1.340(12)

Bond Angles

N1−Co−N2	92.0(2)	N3−Co−O3	86.7(2)
N1−Co−N3	169.4(2)	N4−Co−O3	91.1(2)
N1−Co−N4	103. 6(2)	N5−Co−O3	174.7(3)
N1−Co−N5	94.8(2)	C5−N1−Co	123.4(5)
N2−Co−N3	82.1(2)	C9−N3−Co	118.0(5)
N2−Co−N4	164.4(2)	N2−C8−O1	127.3(8)
N2−Co−N5	94.2(3)	N4−C14−O2	125.9(7)
N3−Co−N4	82. 6(2)	N1−C5−C4	119.8(8)
N3−Co−N5	94.4(2)	N2−C7−C6	109.5(6)
N4−Co−N5	83.9(3)	N3−C13−C12	119.2(7)
N1−Co−O3	84.7(2)	C1−N1−C5	119.2(7)
N2−Co−O3	91.2(2)	O2−C14−C13	121.1(7)

$[Co(Py_3P)(OO^tBu)] \cdot 2CH_2Cl_2$ (**8**)

Bond Distances

Co−N1	1.960(3)	C14−O2	1.245(5)
Co−N2	1.921(3)	O4A−C22	1.442(6)
Co−N3	1.852(3)	O4B−C22	1.525(12)
Co−N4	1.959(3)	C8−C9	1.513(6)
Co−N5	2.024(3)	C12−C13	1.386(6)
Co−O(3A)	1.897(4)	C13−C14	1.502(6)
Co−O(3B)	1.930(4)	C22−C23A	1.515(7)
N1−C1	1.344(5)	C22−C23B	1.490(2)
N2−C7	1.459(5)	C22−C24A	1.563(8)
N5−C17	1.363(5)	C22−C24B	1.460(2)
O3A−O4A	1.515(7)	C22−C25	1.522(6)
O3B−O4B	1.420(2)	Cl1−C26	1.775(5)
O1−C8	1.251(5)	Cl2−C26	1.769(5)

Bond Angles

N1−Co−N2	93.77(14)	O4B−O3B−Co	112.6(12)
N1−Co−N3	171.57(14)	C1−N1−Co	117.0(3)
N1−Co−N4	102. 48(14)	C7−N2−Co	122.9(3)
N1−Co−N5	94.20(14)	C9−N3−Co	117.8(3)
N2−Co−N3	82.11(14)	C14−N4−Co	115.5(3)
N2−Co−N5	93.55(14)	N4−C14−C13	111.1(3)
N3−Co−N4	82.10(14)	N4−C15−C16	110.4(8)
N3−Co−N5	93.40(14)	O1−C8−N2	128.3(4)
N4−Co−N5	82.81(14)	O1−C8−C9	121.1(4)
N1−Co−O3A	85.6(2)	O4B−C22−C25	108.3(6)
N1−Co−O3B	81.2(6)	C1−N1−C5	119.1(4)
N2−Co−O3A	94.8(2)	C5−C6−C7	111.4(3)
N2−Co−O3B	91.2(7)	C11−C10−C9	118.4(4)
N3−Co−O3A	87.4(2)	C23A−C22−C24A	108.0(5)
N3−Co−O3B	91.5(6)	C24A−C22−C25	112.5(4)
O4A−O3A−Co	111.0(4)	Cl1−C26−Cl2	111.1(3)

Py_3PH_2 exhibits its ν_{CO} at 1654 cm^{-1}. In complexes **6**−**8**, ν_{CO} shifts to lower energy and appears in the narrow range of 1590−1596 cm^{-1}. This lowering of stretching frequency results from localization of greater electron density at the deprotonated amido nitrogen, a situation that is represented by the resonance structure **b**. A similar shift of ν_{CO} has been noted in Fe(III) complexes

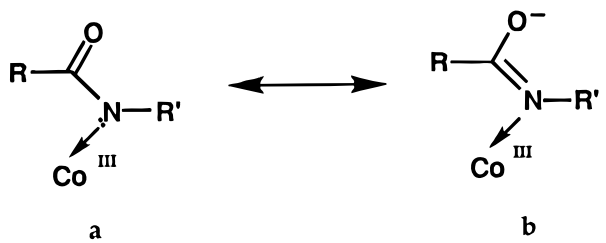

a **b**

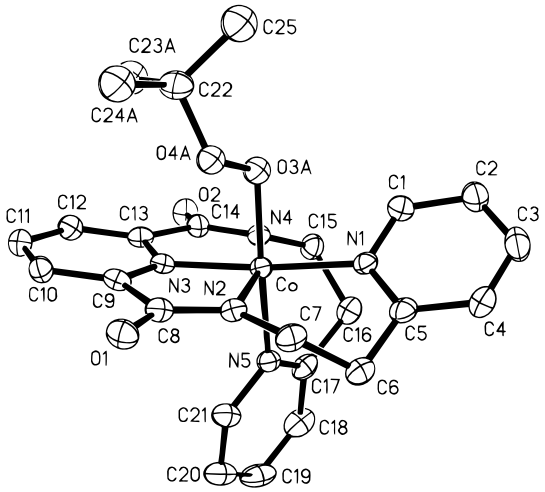

Figure 2. Computer-generated thermal ellipsoid (probability level 50%) plot of $[Co(Py_3P)(OO^tBu)]$ (**8**) with the atom-labeling scheme. Hydrogen atoms are omitted for clarity. Also, only set A of the disordered ^{t}BuOO group (occupancy level 0.75) is shown for the sake of clarity. For a total view of the disordered ^{t}BuOO group, see Figure S1 in the Supporting Information.

with deprotonated amido nitrogen donors in the first coordination sphere.[24] The IR spectra of the reported *tert*-butylperoxy complexes show characteristic bands at 2970−2980 cm^{-1} (ν_{C-H}), 1180−1190 cm^{-1} (ν_{C-C}), and 870−880 cm^{-1} (ν_{O-O}).[8] Complex **8** exhibits bands at 2973, 1192, and 879 cm^{-1} which are all associated with the coordinated ^{t}BuOO$^-$ group.

Electronic Absorption Spectra. The greenish brown color of **6** in water arises from an absorption with λ_{max} at 588 nm (pH = 4, ϵ = 73 M^{-1} cm^{-1}). The absorption presumably arises from the $^1A_1-{}^1E$ transition of the low-spin d^6 Co(III) center. This assignment is supported by the red shift of the band when the coordinated water molecule is replaced by another solvent molecule such as methanol (λ_{max} = 638 nm) or DMSO (λ_{max} = 647 nm). In aqueous solution, the absorption spectrum of **6** also changes with pH. The greenish brown color changes to reddish brown as the pH is increased. At pH = 9, the absorption spectrum of **6** is identical to that of **7** (vide infra).

Although **7** is a neutral complex, it dissolves readily in water to give a reddish brown solution. Such a solution exhibits its electronic absorption as a shoulder at 560 nm. In aqueous solution, **7** also has a strong absorption band at 317 nm (ϵ = 1400 M^{-1} cm^{-1}). The pH of the aqueous solution of **7** is ∼8. When the pH is lowered to ∼4, the absorption spectrum of **7** changes to that of **6**.

Interconversion of $[Co(Py_3P)(H_2O)]ClO_4 \cdot H_2O$ (6) with $[Co(Py_3P)(OH)]$ (7). Changes in the electronic absorption spectrum of **6** with pH in aqueous solution at 25 °C are shown in Figure 3. As the pH is increased from 4 to 9, the absorption at 588 nm diminishes with the concomitant formation of a new shoulder at 560 nm and a band at 317 nm (not shown). The formation of a neutral species in such a solution is evident in its inability to bind to a cation exchange resin (Na^+ form). This transformation is *reversible* and arises from the removal of a proton from the ligated water (eq 1). Results of pH titration (inset of Figure 3) yield a pK_a value of 7 for the coordinated water in **6**.

$$[Co^{III}(Py_3P)(H_2O)]^+ \underset{H^+}{\overset{OH^-}{\rightleftharpoons}} [Co^{III}(Py_3P)(OH)] + H_2O \quad (1)$$

NMR Spectra. The ^1H and ^{13}C NMR spectra of **6** and **7** were recorded in D_2O, and the peaks corresponding to the various hydrogen and carbon atoms of the complexes were

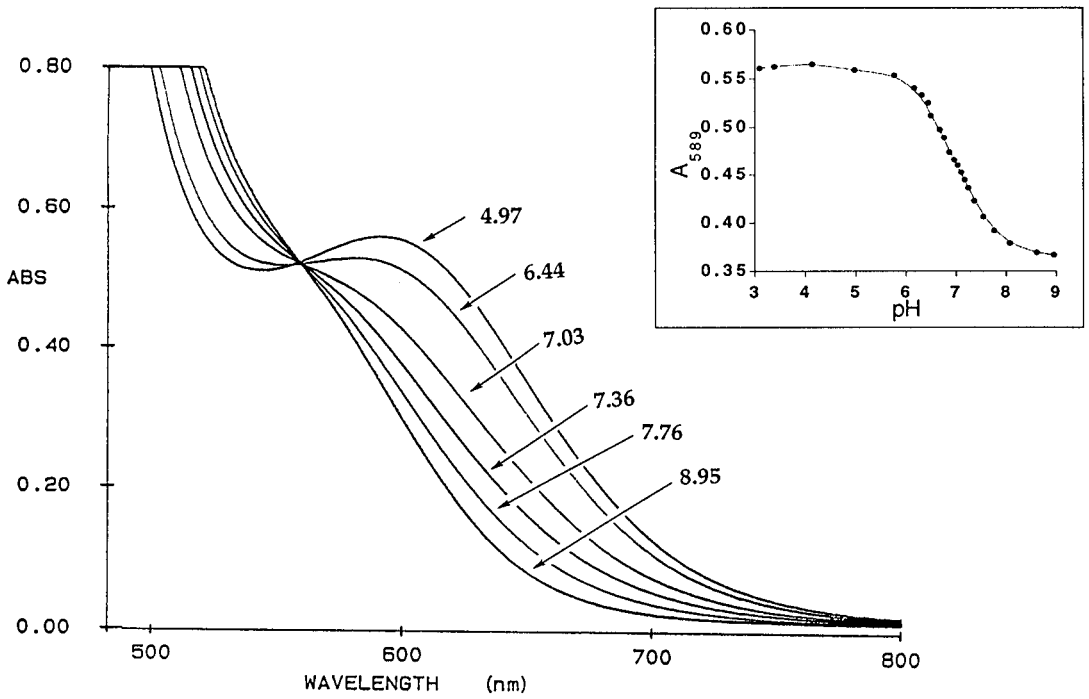

Figure 3. Changes in the electronic absorption spectrum of **6** with pH monitored in aqueous solution. Inset: Plot of pH vs absorbance at 589 nm.

assigned. The NMR spectra of both **6** and **7** in D_2O reveal that the H's attached to the −C6−C7− and −C15−C16− regions are nonequivalent, a fact that implies no free rotation around these bonds. The ligand framework around Co(III) thus appears to be quite rigid in these complexes. The NMR spectra also confirm that addition of 1 equiv of NaOD to a solution of **6** in D_2O affords **7** quantitatively.

The ^1H and ^{13}C NMR spectra of **8** were recorded in $CDCl_3$, and the various resonances were assigned. In $CDCl_3$, the chemical shifts of the ligand protons and carbons of **7** and **8** are very comparable (**6** is sparingly soluble in $CDCl_3$). The presence of the ligated ^{t}BuOO$^-$ group in **8** is indicated by a sharp singlet resonance at 0.52 ppm. A similar upfield shift (the methyl groups of free TBHP resonate at 1.20 ppm in $CDCl_3$) due to interaction of the methyl groups with ring currents of the ligand framework has been reported by Weiss and coworkers.[10] As seen in the crystal structure of **8** (Figure 2), the methyl groups of the coordinated ^{t}BuOO$^-$ group are indeed positioned above the central pyridine ring (the one containing N3). If such a disposition persists in solution, then shielding of the methyl groups of the ligated ^{t}BuOO$^-$ group is expected.

Structure and Reactivity of [Co(Py$_3$P)] (9). Under strictly anaerobic conditions, reactions of Co(II) salts with Py_3PH_2 in the presence of 2 equiv of a strong base afford the neutral Co(II) complex [Co(Py_3P)] (**9**), in which the deprotonated Py_3P^{2-}

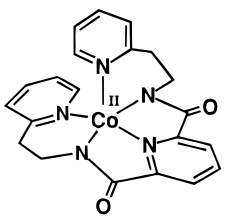

Structure of [Co(Py_3P)] (**9**)

ligand is coordinated to the Co(II) center in a pentadentate fashion. The burgundy color in MeOH results from an absorption with λ_{max} at 440 nm. This color develops only when the base is added.[25] Also, the EPR signal of **9** (Figure 4) is not fully generated until 2 equiv of a strong base is added. The structure of **9** was assigned on the basis of its EPR spectrum

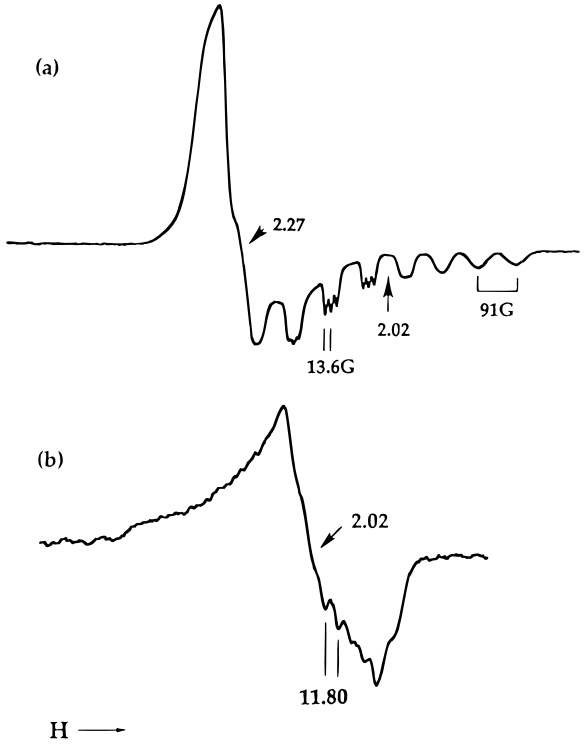

Figure 4. X-Band EPR spectra of (a) [Co^{II}(Py_3P)] and (b) [Co^{III}(Py_3P)(O_2^-)] in methanol glass at 100 K. Selected *g* and *A* values are indicated in the spectra. Spectrometer settings: microwave frequency, 9.43 GHz; microwave power, 13 mW; modulation frequency, 100 KHz; modulation amplitude, 2 G.

(25) Although [Cu(Py_3P)][15] is synthesized from copper(II) acetate and Py_3PH_2 (acetate ions in methanol act as the base in such reactions), formation of [Co(Py_3P)] requires a much stronger base. This suggests that Cu(II) promotes deprotonation of amide NH groups more readily than Co(II). Also see: Sundberg, R. J.; Martin, R. B. *Chem. Rev.* **1974**, *74*, 471.

Table 5. Stoichiometric Oxidation of Cyclohexane by $[Co(Py_3P)(OO^tBu)]\cdot 2CH_2Cl_2$ (**8**)[a]

Time Profile[b,c]

time, h	% **A**	% **K**	% **C**	% total
0.5	1.6	5.0	0	6.6
1.0	2.3	6.3	1.0	9.6
2.0	6.8	18.0	2.4	27.2
3.0	14.4	21.1	4.3	39.8
4.0	18.0	25.0	4.8	47.8
5.0	23.4	22.6	7.1	53.1
7.0	27.0	24.6	7.2	58.8

Temperature Profile[b,d]

T, °C	% **A**	% **K**	% **C**	% total
50	0.6	1.9	0	2.5
60	2.3	7.7	1.2	11.2
70	6.8	18.0	5.8	30.6
80	18.8	23.0	10.1	51.9
90	16.3	26.0	8.1	50.4
100	4.7	19.4	8.2	32.3

[a] Yields based on **8**. [b] Reaction mixtures consisted of 0.5 mL of CH_2Cl_2, 0.5 mL of CyH, and **8**. [c] Reaction temperature was 70 °C. [d] Reaction time was 2 h.

(Figure 4a). **9** displays a nearly axial EPR spectrum with eight-line hyperfine splitting in the $g_{||}$ region due to ^{59}Co ($I = {}^7/_2$) nucleus. This EPR feature is characteristic of low-spin d^7 ($S = {}^1/_2$) Co(II) in 5-coordinate square pyramidal geometry with the unpaired electron in the d_{z^2} orbital.[26] The presence of one axial N ($I = 1$) donor gives rise to the three-line superhyperfine splitting in the parallel region. The EPR parameters of **9** ($g_\perp = 2.27$, $g_{||} = 2.02$, $A_{||}^{Co} = 91$ G, $A_{||}^{N} = 13.6$ G) are typical of 5-coordinate square pyramidal complexes.[26−28]

Reduction of structurally characterized $[Co(Py_3P)(H_2O)]ClO_4\cdot H_2O$ (**6**) with lithium triethylborohydride also affords **9** (confirmed by EPR spectroscopy). This provides further evidence in favor of the proposed structure of **9**. The EPR spectrum of **9** transforms dramatically upon exposure to O_2 (Figure 4b). The axial ($g_\perp > g_{||}$) EPR signal of **9** changes to the more symmetrical ($g_{||} > g_\perp$) signal at $g \approx 2$, and the $A_{||}^{Co}$ value drops to 11.8G. This latter fact suggests that the unpaired electron density resides mostly on the dioxygen moiety in the oxygenated species. The EPR spectrum of the oxygenated species (Figure 4b) is typical of monomeric Co(III) superoxide complexes[26,27] and identifies it as $[Co^{III}(Py_3P)(O_2^-)]$. This assignment is further confirmed by the fact that the same EPR spectrum is obtained when **6** is allowed to react with K(crown)-O_2 in methanol.

Oxidation of Cyclohexane by [Co(Py$_3$P)(OO^{t}Bu)] (8). Thermal decomposition of **8** in dichloromethane solution[29] in the presence of cyclohexane (CyH) affords cyclohexanol (**A**), cyclohexanone (**K**), and cyclohexyl chloride (**C**) in significant yields. As seen in Table 5, a maximum total yield of 59% (based on **8**) of the oxidized products is obtained under optimum conditions. The oxidizing capacity of **8** thus appears superior compared to that of the [Co(BPI)(OCOR)(OOR′)] complexes reported by Weiss.[8] When the yields of the oxidation reactions are monitored as a function of temperature, it becomes evident that substrate oxidation is not significant at temperatures below

Scheme 1

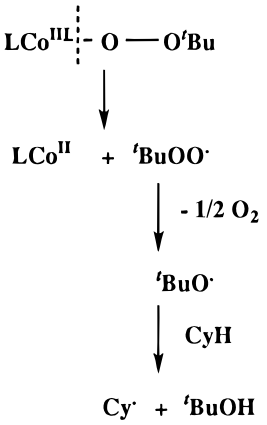

50 °C. A linear increase in yields of the oxidized product is seen from 50 to 80 °C (Table 5). Further increase in temperature results in diminished yields of all products. The time profile of the oxidation reaction (Table 5) at 70 °C shows a gradual increase in product formation with maximum yield at about 7 h. Interestingly, when **8** is heated with cyclohexane in dichloromethane solution under strictly anaerobic conditions, **C** is the only product. It is therefore evident that molecular oxygen which is present in the reaction vessel and dissolved in the solvents is a critical participant in the mechanism of cyclohexane oxidation by **8**.

The fate of **8** in the reaction mixture during cyclohexane oxidation has been monitored with the aid of electronic absorption spectroscopy. As the reaction progresses, one observes a steady decrease in the absorbance at 645 nm with concomitant increase in absorbance at 317 nm. At the end of the reaction, the final spectrum is identical to that of $[Co(Py_3P)(OH)]$ (**7**) although the absorbances of the bands indicate partial destruction (∼15%) of the cobalt complex.[30] Since **7** is rapidly converted into **8** in dichloromethane in the presence of dry TBHP (NMR evidence), one expects that a catalytic system could be obtained with **8** and excess TBHP. Indeed, when the oxidation of cyclohexane is carried out with **8** + TBHP, increased yields of the oxidized products confirm many turnovers (vide infra).

Mechanism of Cyclohexane Oxidation by 8. The mechanism of cyclohexane oxidation initiated by thermal decomposition of **8** could involve the homolytic cleavage of either the $Co^{III}-O$ bond (Scheme 1) or the O−O bond (Scheme 2) of $[Co(Py_3P)(OO^tBu)]$ and the subsequent alkane activation step by H atom abstraction from the substrate (CyH) to form the cyclohexyl radical (Cy•). In dichloromethane solution, Cy• is readily converted into **C.** Formation of **C** therefore implies Cy• formation in our reactions.[32] It is important to note that homolysis of the O−O bond in **8** affords ^{t}BuO• (Scheme 2), while homolytic cleavage of the $Co^{III}-O$ bond produces ^{t}BuOO• (Scheme 1) in the reaction mixture. Out of these two species, only ^{t}BuO• has sufficent radical strength (a thermodynamic

(26) Jones, R. D.; Summerville, D. A.; Basolo, F. *Chem Rev.* **1979**, *79*, 139.
(27) Smith, T. D.; Pilbrow, J. R. *Coord. Chem. Rev.* **1981**, *39*, 295.
(28) Farinas, E.; Baidya, N.; Mascharak, P. K. *Inorg. Chem.* **1994**, *33*, 5970.
(29) Since **8** is insoluble in pure cyclohexane, one needs dichloromethane to solubilize the complex in the oxidation medium. After several attempts in mixed solvents of different ratios, a 1:1 mixture of cyclohexane and dichloromethane was found to be optimal for this work.
(30) At the end of the oxidation reaction, a small amount of insoluble precipitate is observed at the bottom of the reaction vessel.
(31) Trapping of cyclohexyl radicals by halogenated hydrocarbons has been noted in cyclohexane oxidation: (a) Leising, R. A.; Kojima, T.; Que, L., Jr. In *The Activation of Dioxoygen and Homogeneous Catalytic Oxidation*; Barton, D. H. R., Martell, A. E., Sawyer, D. T., Eds.; Plenum Press: New York, 1993; pp 321−331. (b) Kim, J.; Larka, E.; Wilkinson, E. C.; Que, L., Jr. *Angew. Chem., Int. Ed. Engl.* **1995**, *34*, 2048.
(32) Barton, D. H. R.; Sawyer, D. T. In *The Activation of Dioxygen and Homogeneous Catalytic Oxidation*; Barton, D. H. R., Martell, A. E., Sawyer, D. T., Eds.; Plenum Press: New York, 1993; p 4.

Scheme 2

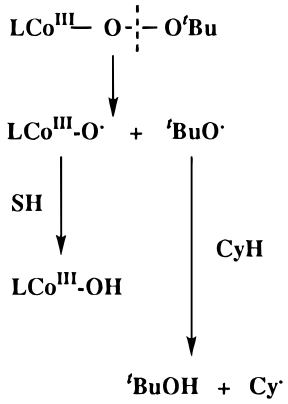

parameter for the formation of ^{t}BuOH from the ^{t}BuO$^\bullet$ radical), 97 kcal mol^{-1}, to abstract hydrogen from cyclohexane, which has a C−H bond dissociation energy of 95 kcal mol^{-1}.[33] ^{t}BuOO$^\bullet$, on the other hand, does not have sufficient radical strength (83 kcal mol^{-1}) to abstract an H atom from cyclohexane. However, ^{t}BuO$^\bullet$ can be generated via decomposition of the ^{t}BuOO$^\bullet$ radical.[33] Thus, both schemes can afford ^{t}BuO$^\bullet$, the radical species responsible for H atom abstraction from cyclohexane. The one key result that provides strong evidence in favor of O−O bond cleavage in **8** (Scheme 2) is the complete absence of the mixed peroxide CyOO^{t}Bu (**P**) as a product of the oxidation (Table 5). One expects this mixed peroxide if ^{t}BuOO$^\bullet$ radicals are present in the reaction mixture (formed via Cy$^\bullet$ and ^{t}BuOO$^\bullet$ radical combination). It is thus evident that thermal decomposition of **8** proceeds via homolysis of the O−O bond and cyclohexane oxidation is promoted by the ^{t}BuO$^\bullet$ fragment, a product of the homolysis. The presence of ^{t}BuO$^\bullet$ in the reaction mixture is further confirmed by detection of methanol and acetone as additional products of the oxidation by **8**.[34a] The less-than-stoichiometric yield of oxidation products may be attributed to the loss of ^{t}BuO$^\bullet$ by this decompostion pathway, thus lowering the amount of Cy$^\bullet$ formation. The decrease in total yields of **A**, **K**, and **C** for reactions at temperatures higher than 80 °C perhaps can be explained in terms of higher rates of decompostion of ^{t}BuO$^\bullet$.

As mentioned earlier, the formation of **A** and **K** is dependent on the presence of O_2. This dependence, together with the approximately 1:1 ratio of **A**:**K** obtained at the end of longer reaction times (>4 h), suggests that the production of **A** and **K** in the present reactions could be derived from a Russell-type reaction. This reaction involves combination of Cy$^\bullet$ and O_2 to form CyOO$^\bullet$, which subsequently terminates to give **A** and **K** (eq 2).[35] Trapping of Cy$^\bullet$ by dichloromethane produces **C**, the

$$2\mathrm{Cy}^\bullet + 2\mathrm{O}_2 \rightarrow 2\mathrm{CyOO}^\bullet \rightarrow \mathbf{A} + \mathbf{K} + \mathrm{O}_2 \qquad (2)$$

third product of the oxidation reaction. In complete absence of O_2, **C** becomes the only product presumably due to efficient trapping of the Cy$^\bullet$ radicals by dichloromethane which is present in a large amount in the reaction mixture. It is important to note that if ^{t}BuOO$^\bullet$ were present in the reaction mixture (i.e., if Scheme 1 were operative), then O_2 derived from ^{t}BuOO$^\bullet$ (reactions 3−5)[34b,c] would have afforded some **A** and **K** even

$$^t\mathrm{BuO}^\bullet + {}^t\mathrm{BuOO}^\bullet \longrightarrow {}^t\mathrm{BuOO}{}^t\mathrm{Bu} + 1/2\,\mathrm{O}_2 \quad (3)$$

$$^t\mathrm{BuOO}^\bullet \longrightarrow {}^t\mathrm{BuO}^\bullet + 1/2\,\mathrm{O}_2 \quad (4)$$

$$2\ {}^t\mathrm{BuOO}^\bullet \rightarrow {}^t\mathrm{BuOOOO}{}^t\mathrm{Bu} \rightarrow {}^t\mathrm{BuOOO}{}^t\mathrm{Bu} + 1/2\,\mathrm{O}_2 \quad (5)$$

under strictly anaerobic conditions. Detection of **C** as the only oxidation product under strictly anaerobic conditions therefore supports Scheme 2 as the operating mechanism of cyclohexane oxidation by **8**.

Cleavage at the O−O bond (Scheme 2) results in formation of [(Py$_3$P)Co^{III}O$^\bullet$] and ^{t}BuO$^\bullet$. Since we recover **7** at the end of the oxidation reaction and detect less-than-expected amounts of cyclohexanol at the early stages of the oxidation (Table 5), it appears that [(Py$_3$P)Co^{III}O$^\bullet$] abstracts an H atom from cyclohexanol to generate **7** in the reaction mixture. Such a reaction also explains the more-than-expected amounts of cyclohexanone one obtains at the early stages of oxidation (Table 5). Since the identity of the species that provides the H atom to [(Py$_3$P)Co^{III}O$^\bullet$] has not been established unambiguously in the present work, it is denoted as SH in Scheme 2.

Homolysis of the Co^{III}−O bond in **8** (Scheme 1) is not favored partly due to the fact that the strong-field ligand Py$_3$P^{2-}, with two deprotonated amido nitrogen donors, offers more stabilization to cobalt in the +3 oxidation state. Since coordination of Py$_3$P^{2-} to Co(II) raises an electron to a highly destabilized orbital, [Co^{II}(Py$_3$P)] (**9**) is quite reactive and is readily oxidized. It is therefore not surprising that one recovers **7**, a Co(III) species, as the decomposition product of **8**. That no Co(II) species is formed in the reaction mixture during cyclohexane oxidation is confirmed by the fact that aliquots of the reaction mixtures, removed at different intervals, all display sharp NMR resonances.

Quite in contrast, decomposition of the Co(III) peroxo complex [Co(salen)(OO^{t}Bu)] (**4**) in the presence of cyclohexane (60 °C, 3 h, solvent dichloromethane/cyclohexane) affords **P** (7.5%) in addition to **A** (10.4%), **K** (15.8%), and **C** (7.6%). The products of this oxidation reaction suggest that the decomposition of **4** proceeds via Co^{III}−O bond homolysis (Scheme 1).[36] As expected, one obtains [Co^{II}(salen)] from this reaction mixture at the end of the oxidation. The presence of **P** in the products clearly indicates that ^{t}BuOO$^\bullet$ is present in the reaction mixture in this case. The driving force for the Co−O bond homolysis in this case is the formation of thermodynamically stable [Co^{II}(salen)]; the weaker (compared to Py$_3$P^{2-}) salen^{2-} ligand does stabilize the Co(II) center and hence homolysis of the Co−O bond in **4** is preferred. Collectively, these results demonstrate that the ligand L in the [LCo^{III}−O−O−R] species plays a crucial role in promoting Co^{III}−O vs O−O bond cleavage and hence the distribution of the oxidized products.

The observation that, in single-turnover, oxidation of cyclohexane with **8** affords **7** as the final cobalt-containing species prompted us to study the catalytic oxidation of cyclohexane with **8** and excess (30 equiv) TBHP. Indeed, in dichloromethane/cyclohexane medium, **8** produces more oxidized products in the presence of excess TBHP. For example, at 80 °C, **8** + 30 equiv of TBHP produces, within 2 h, 310% **A**, 210% **K**, and

(33) (a) Ingold, K. U. In *Free Radicals*, Vol. 1; Kochi, J. K., Ed.; John Wiley & Sons: New York, 1973; p 59. (b) Howard, J. A. *Adv. Free Radical Chem.* **1971**, *4*, 49.

(34) (a) Almarsson, O.; Bruice, T. C. *J. Am. Chem. Soc.* **1995**, *117*, 4533. (b) Minisci, F.; Fontana, F.; Araneo, S.; Recupero, F.; Banfi, S.; Quici, S. *J. Am. Chem. Soc.* **1995**, *117*, 226. (c) Milas, N. A.; Plesnicar, B. *J. Am. Chem. Soc.* **1968**, *90*, 4450.

(35) Russell, G. A. *J. Am. Chem. Soc.* **1957**, *79*, 3871.

(36) Cleavage of the Co^{III}−OO^{t}Bu bond in [Co(salen)(OO^{t}Bu)] is partly assisted by dichloromethane. See: Nishinaga, A.; Forster, S.; Eichhorn, E.; Speiser, B.; Rieker, A. *Tetrahedron Lett.* **1992**, *33*, 4425.

10% **C** as the oxidized products.[37,38] The yields correspond to at least five turnovers and thus confirm catalytic oxidation of cyclohexane. Interestingly, **7** also promotes catalytic oxidation of cyclohexane in the presence of TBHP. The latter result indicates formation of **8** from **7** + TBHP, a reaction which is also supported by the NMR data. At this time, we are actively pursuing these catalytic reactions in order to establish the mechanism(s) of catalytic hydrocarbon oxidation by Co(III) complexes and hydroperoxides.

Summary and Conclusions

The following are the principal results and conclusions of this investigation.

(i) Three cobalt complexes (**6**−**8**) of the strong-field ligand Py_3PH_2 have been synthesized, and two of these complexes, **6** and **8**, have been structurally characterized. In all three complexes, the ligand employs two deprotonated amido nitrogens and three pyridine ring nitrogens as the donor centers. The sixth ligand in **6**−**8** is H_2O, OH^- and ^{t}BuOO$^-$, respectively.

(ii) In basic media, deprotonation of the coordinated water in **6** affords **7**. The interconversion **6** ↔ **7** is reversible. The pK_a of the coordinated water in **6** is 7.

(iii) [Co(Py_3P)] (**9**) exhibits a nearly axial EPR spectrum which is typical of low-spin Co(II) in 5-coordinate square pyramidal geometry. Exposure of **9** to dioxygen results in formation of the superoxide adduct [$Co^{III}(Py_3P)(O_2^-)$].

(iv) Thermal decomposition of the alkylperoxo complex **8** in the presence of cyclohexane results in oxidation of the hydrocarbon to cyclohexanol (**A**) and cyclohexanone (**K**). This oxidation proceeds via formation of the cyclohexyl radical (Cy·) generated in the reaction of cyclohexane with ^{t}BuO•. The ^{t}BuO• radical results from homolysis of the O−O bond in **8**. The presence of ^{t}BuO• in the reaction mixture is supported by the detection of methanol and acetone in the products, while the presence of Cy• is indicated by the formation of significant amounts of cyclohexyl chloride (**C**). The absence of the mixed peroxide CyOO^{t}Bu (**P**) in the products suggests that no ^{t}BuOO• is present in the reaction mixture. Cyclohexanol and cyclohexanone are produced only in the presence of dioxygen presumably via a Russell-type termination reaction. Under strictly anaerobic conditions, Cy• affords **C** as the only product.

(v) The low-spin d^6 electronic configuration of cobalt in [$Co^{III}(Py_3P)(X)$] (X = H_2O, OH^-, ^{t}BuOO$^-$) is stabilized by the strong ligand field of Py_3P^{2-}. Therefore, cleavage occurs selectively at the O−O bond in **8**, a process that keeps the cobalt center in the 3+ oxidation state.

Acknowledgment. Financial support from NIH-MBRS Grant GM08132 and the UCSC SEED fund is gratefully acknowledged.

Supporting Information Available: The total view of the disordered ^{t}BuOO group in **8** (Figure S1) and tables of crystal data and intensity collection and refinement parameters, bond distances and angles, H atom coordinates, and anisotropic and isotropic thermal parameters for **6** and **8** (17 pages). Ordering information is given on any current masthead page.

IC960500M

(37) In the case of catalytic oxidation, one obtains 25% **P** in addition to **A**, **K**, and **C**. It thus appears that when excess TBHP is present in the reaction mixture, the ^{t}BuO• radical abstracts an H atom from TBHP to generate the ^{t}BuOO•. radical which subsequently combines with Cy· to produce **P**.

(38) Oxidation of phenols and related substrates by mixtures of Co(II) salts, Py_3PH_2, and molecular oxygen in DMF was recently reported by Hirao and co-workers: (a) Moriuchi, T.; Hirao, T.; Ishikawa, T.; Ohshiro, Y.; Ikeda, I. *J. Mol. Catal*. **1995**, *95*, L1−L5. (b) Hirao, T.; Moriuchi, T.; Mikami, S.; Ikeda, I.; Ohshiro, Y. *Tetrahedron Lett*. **1993**, *34*, 1031.